EUROPEAN UNION
European Structural and Investment Funds
Operational Programme Research, Development and Education

FZU Institute of Physics of the Czech Academy of Sciences

MINISTRY OF EDUCATION, YOUTH AND SPORTS

AUSTRIAN INSTITUTE OF TECHNOLOGY
TOMORROW TODAY

Optical spectroscopy and biosensors for investigation of biomolecules and their interactions

Jakub Dostalek

AIT - Austrian Institute of Technology GmbH
Biosensor Technologies Unit
Konrad-Lorenz-Strasse 24 | 3430 Tulln | Austria
T +43(0) 664 2351773

FZU – Institute of Physics of the Czech Academy of Sciences,
Na Slovance 1 | Prague 182 00 | Czech Republic
T+420 776767927

jakub.dostalek@ait.ac.at | http://www.ait.ac.at | http://www.jakubdostalek.cz

Non-SPR Optical Biosensors with Direct Detection Format

Content

- Portable SPR biosensors with cell phone readout

- Grating coupler
- Whispering gallery modes sensing,
- Reflectometric interference spectroscopy - RIFS
- Mach Zehnder interferometry-based sensors,
- Surface-enhanced diffraction, scattering, ISCAT.

Portable SPR Biosensors with Direct Readout Format

EUROPEAN UNION
European Structural and Investment Funds
Operational Programme Research,
Development and Education

MINISTRY OF EDUCATION,
YOUTH AND SPORTS

FZU Institute of Physics of the Czech Academy of Sciences

AIT AUSTRIAN INSTITUTE OF TECHNOLOGY

Grating-Coupled SPR

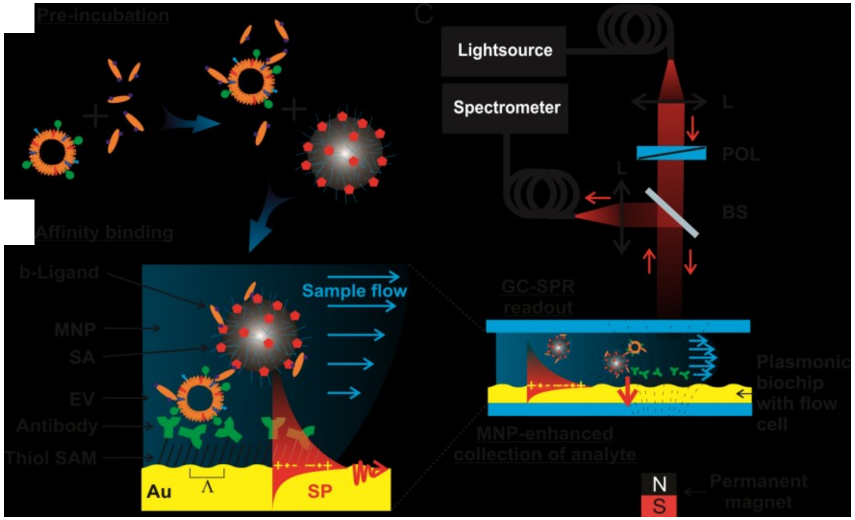

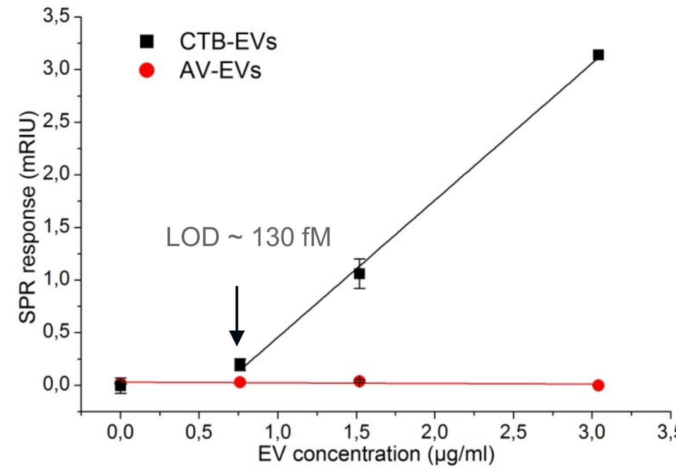

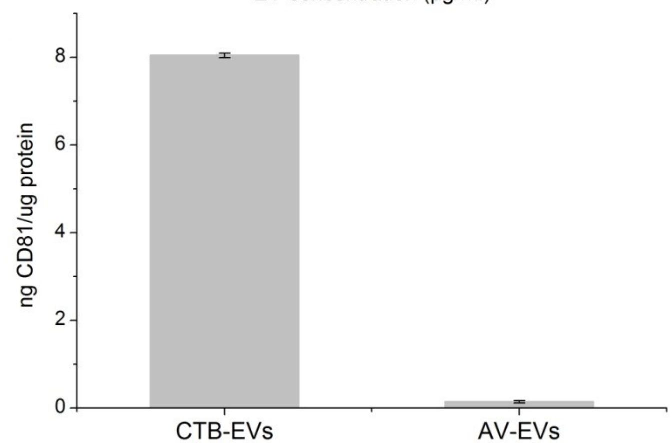

- Detection of exosomes secreted by mesenchymal stem cells.
- Interrogation of sub populations carrying CD81 and lipid binding domains recognized by Annexin V and Cholera toxin B chain
- Step towards ovarian cancer diagnostics by the analysis of blood plasma.

Agnes Reiner, Nicolas Guillermo Ferrer, Priyamvada Venugopalan, Ruenn Chai Lai, Saikiam Lim and Jakub Dostalek, Magnetic nanoparticle-enhanced surface plasmon resonance biosensor for extracellular vesicle analysis, Analyst, 2017, 142, 3913-3921.

Grating-Coupled SPR Biosensor

- Grating coupled SPR allows for design of compact sensors.
- Exploited in the analysis of whole plasma samples with the help of antifouling brush polymer architecture

a) **Compact reader**

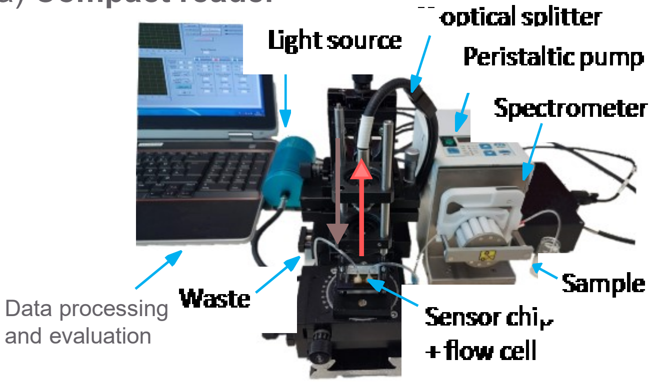

b) **Reflectivity spectra *R*(*λ*)**

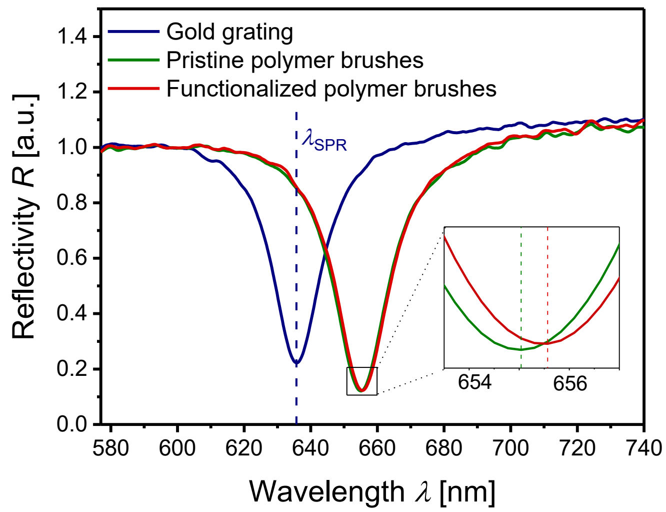

c) **SPR kinetics $\lambda_{SPR}(t)$**

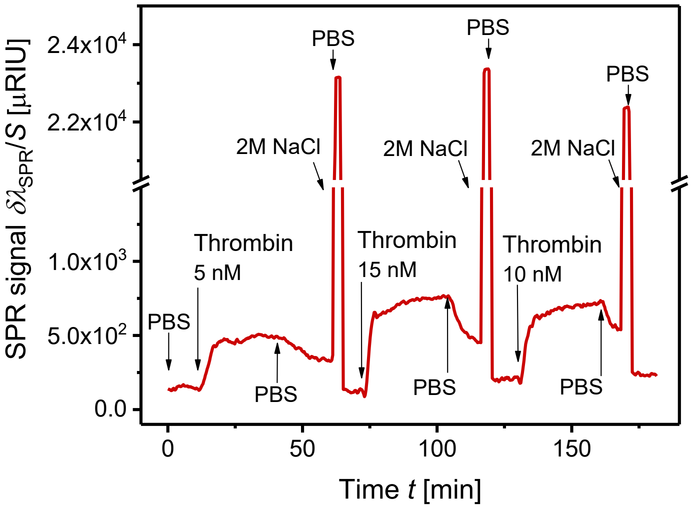

Daria Kotlarek, Mariia Vorobii, Wojciech Ogieglo, Cesar Rodriguez-Emmenegger, Wolfgang Knoll, Jakub Dostálek, Compact grating-coupled plasmonic biosensor for the analysis of thrombin in human blood plasma, 2019, ACS Sensors, 4, 8, 2109-2116.

Cell Phone Readout for SPR Biosensor

- Using cell phone optics holds potential to lift of (arguably) high price of optical systems.

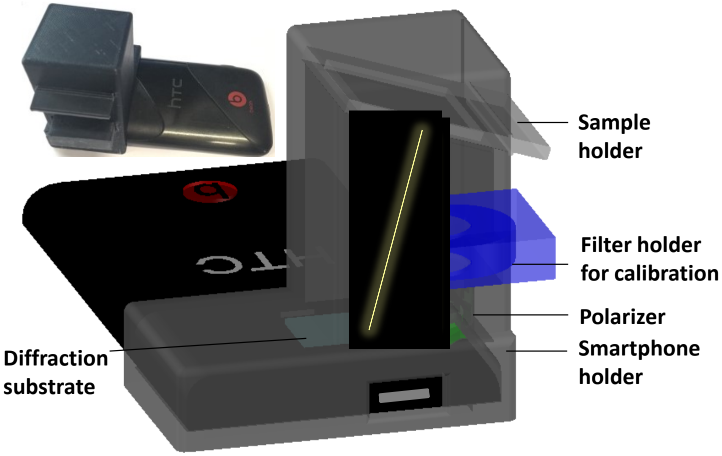

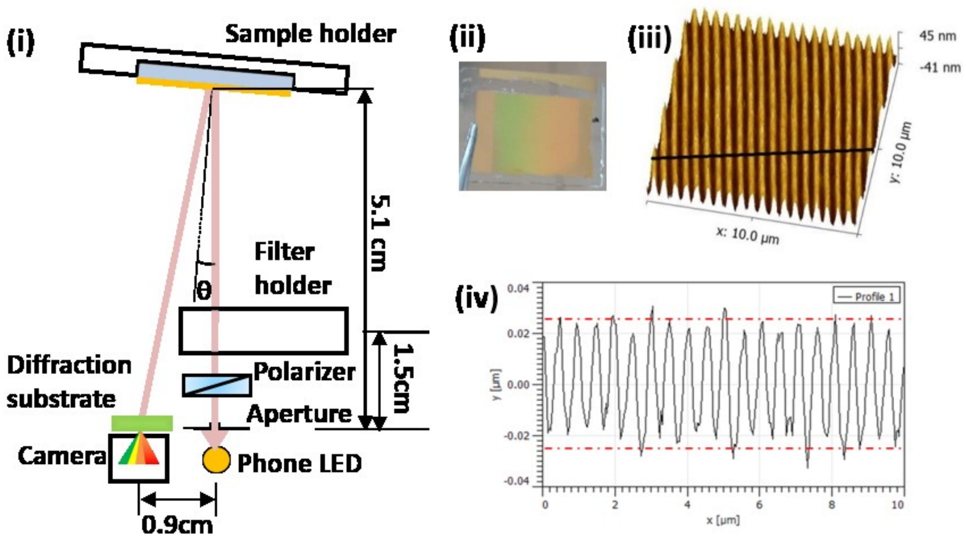

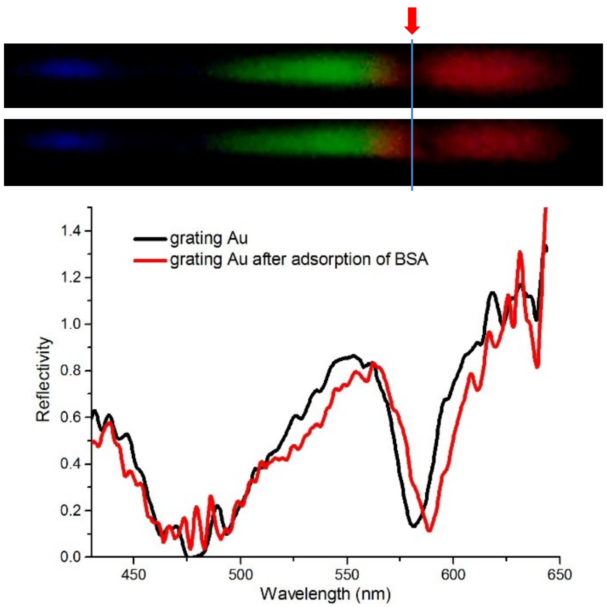

Jinling Zhang, Imran Khan, Zhang Qingwen, Xiaohu Liu, Jakub Dostalek, Bo Liedberg, Yi Wang, Lipopolysaccharides detection on a grating-coupled surface plasmon resonance smartphone biosensor, Biosensors and Bioelectronics, 2018, 99, 312-317.

Diffraction-Coupled SPR with Spectral Dispersive Element

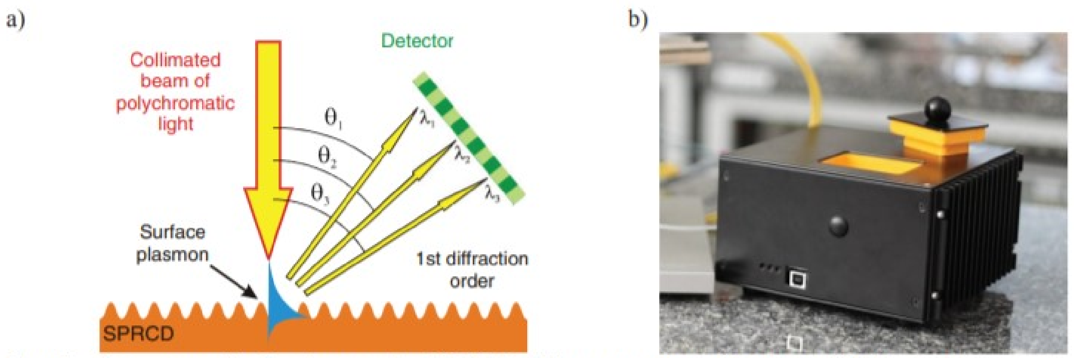

Figure 1: a) Spectroscopy of surface plasmons using SPRCD. b) A laboratory prototype of the compact SPRCD sensor.

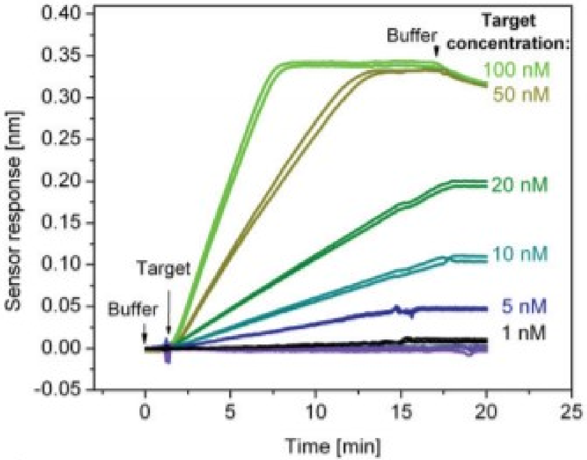

•10.1007/s00216-010-4067-z

- Ultimate simplicity achieved by combining SPR detection and dispersive element on one diffraction grating structure.

O. Telezhnikova, J. Dostálek, J. Homola: Method For Spectroscopy Of Surface Plasmons In Surface Plasmon Resonance Sensors And An Element For The Use Of Thereof, CZ299489, US7973933, CA2598118, CN101175989, JP4999707.

Preparation of Diffraction Grating Structures

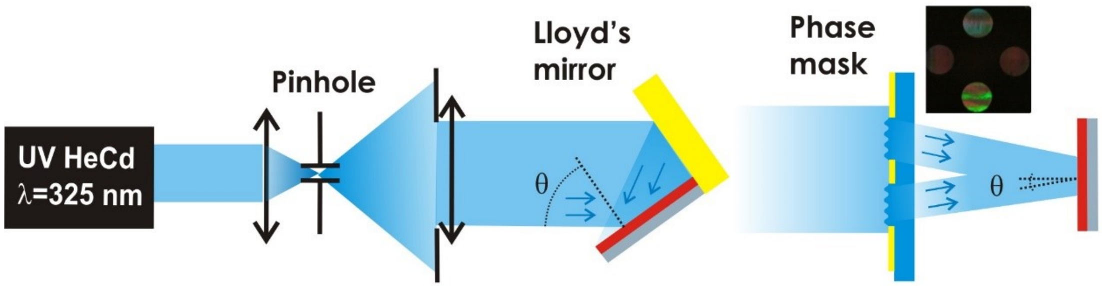

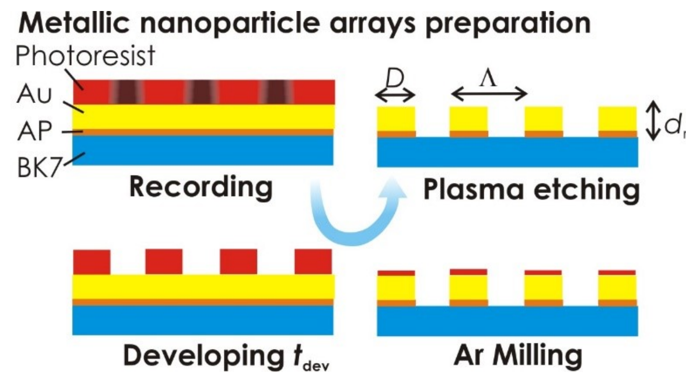

➧ UV laser interference lithography

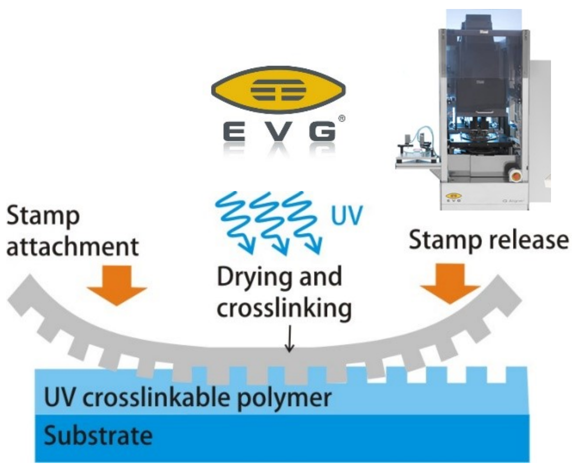

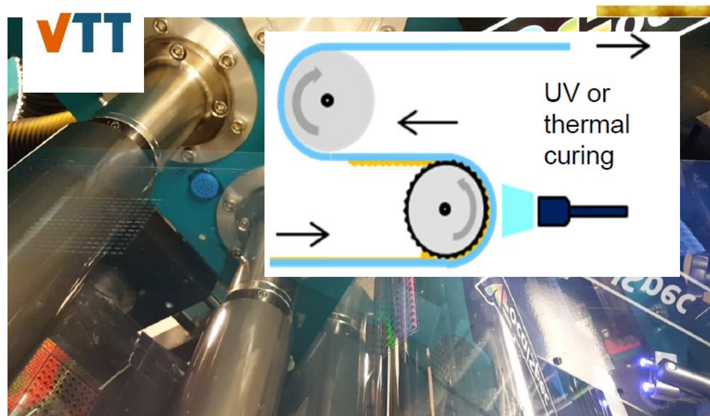

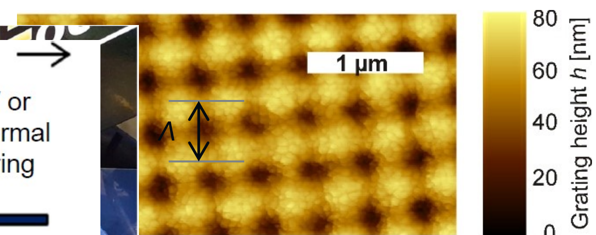

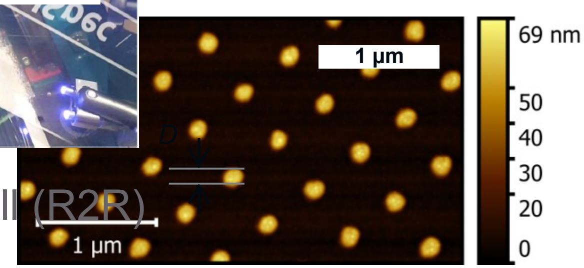

➧ UV nanoimprint lithography with flexible stamp and roll-to-roll (R2R)

Nestor G. Quilis, Mederic Lequeux, Pryiamvada Venugopalan, Imran Khan, Souhir Boujday, Wolfgang Knoll, Marc Lamy de la Chapelle, Jakub Dostalek, Tunable laser interference lithography preparation of plasmonic nanoparticle arrays tailored for SERS, Nanoscale, 2018, 10, 10268-10276

Grating Coupler

Grating Coupler

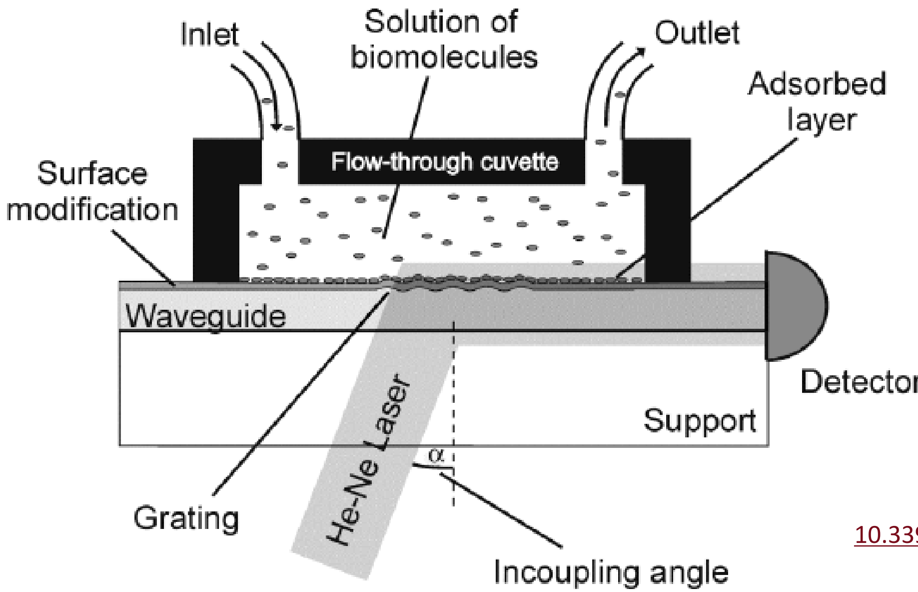

10.3390/bios2040341

- One of original concepts competing with SPR and also referred as to optical waveguide lightmode spectroscopy (OWLS).
- Angular modulation-based direct detection of molecular binding events. Comparable performance as SPR biosensors.

D. Clerc and W. Lukosz, Integrated optical output grating coupler as refractometer and (bio-)chemical sensor, Sensors and Actuators B, 11, (1998) 461-465.

Colorimetric Photonic Crystal

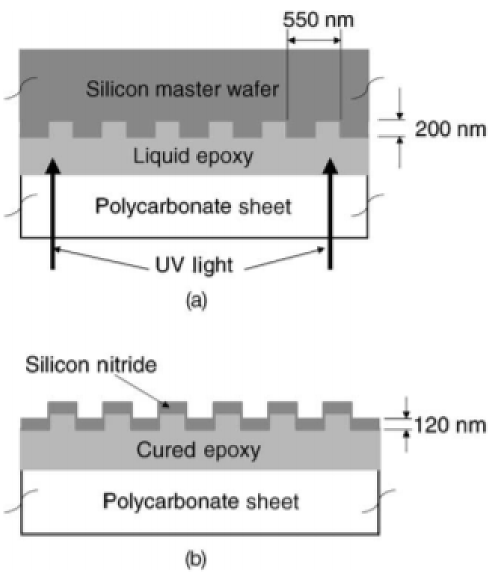

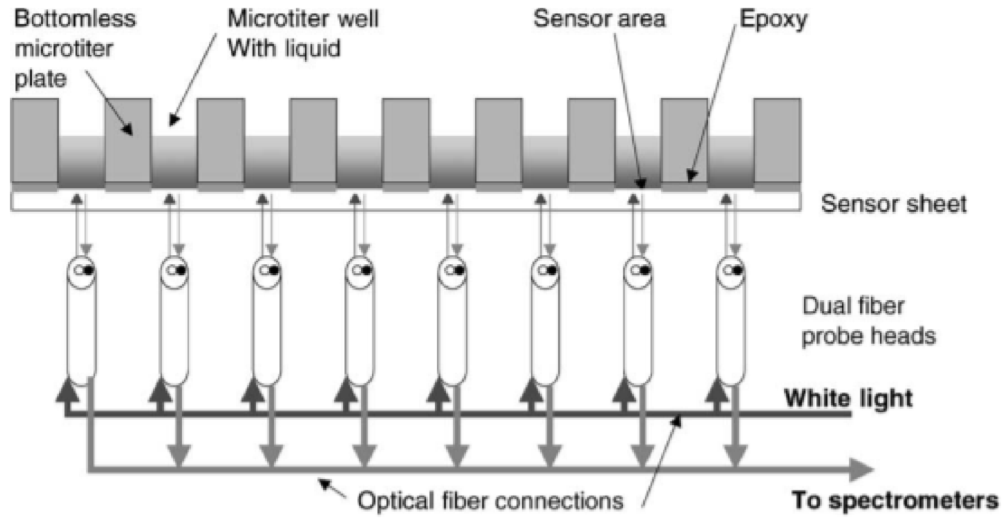

- Dielectric photonic crystal structure acting as a waveguide.
- Wavelength interrogation of resonant coupling detuning.

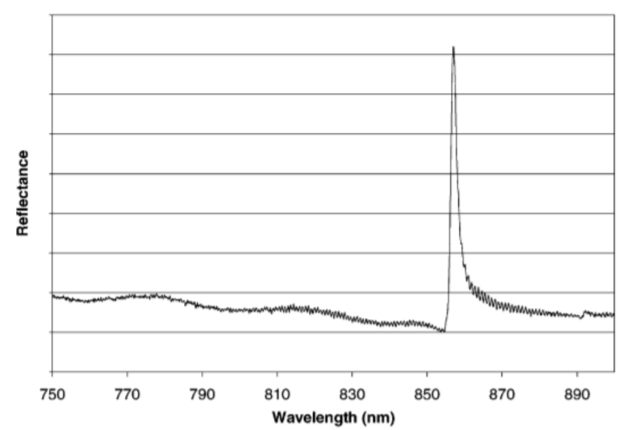

Brian Cunningham, Bo Lin, Jean Qiu, Peter Li, Jane Pepper, Brenda Hugh, A plastic colorimetric resonant optical biosensor for multiparallel detection of label-free biochemical interactions, Sensors and Actuators B: Chemical, 2002, 85/3, 219-226.

Colorimetric Photonic Crystal

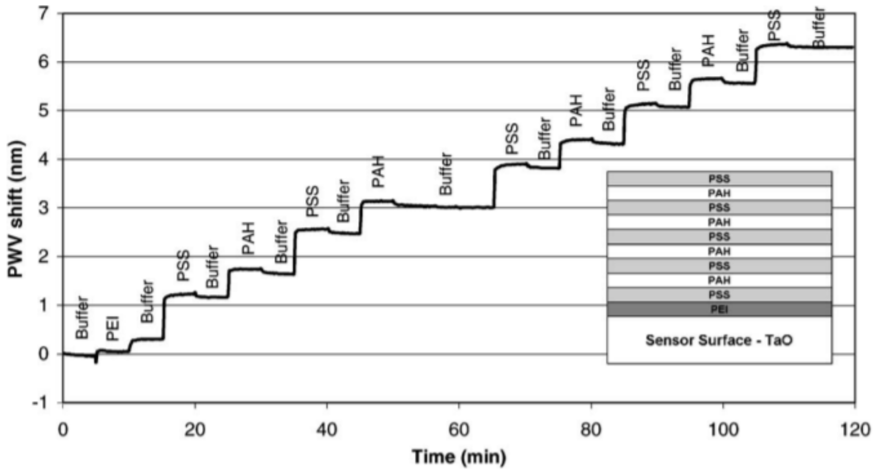

Brian Cunningham, Bo Lin, Jean Qiu, Peter Li, Jane Pepper, Brenda Hugh, A plastic colorimetric resonant optical biosensor for multiparallel detection of label-free biochemical interactions, Sensors and Actuators B: Chemical, 2002, 85/3, 219-226.

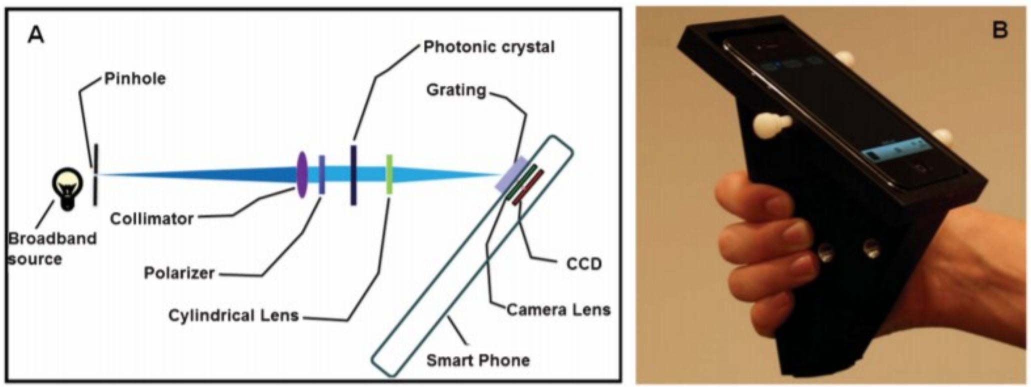

Dustin Gallegos, Kenneth D Long, Hojeong Yu, Peter P Clark, Yixiao Lin, Sherine George, Pabitra Nath, Brian T Cunningham, Lab on a Chip, 2013, 13/11, 2124-2132.

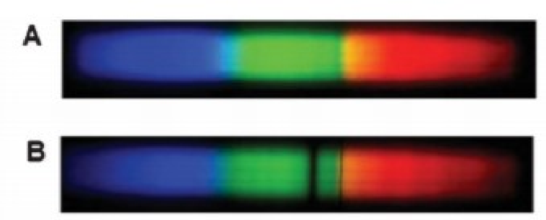

Whispering Gallery Modes

Ring Resonators

Optical micro-resonators that exhibit a large Q-factor and small modal volume V (large Q/V) - highest sensitivity for label-free detection of molecules. Single-molecule detection capability is prospected.

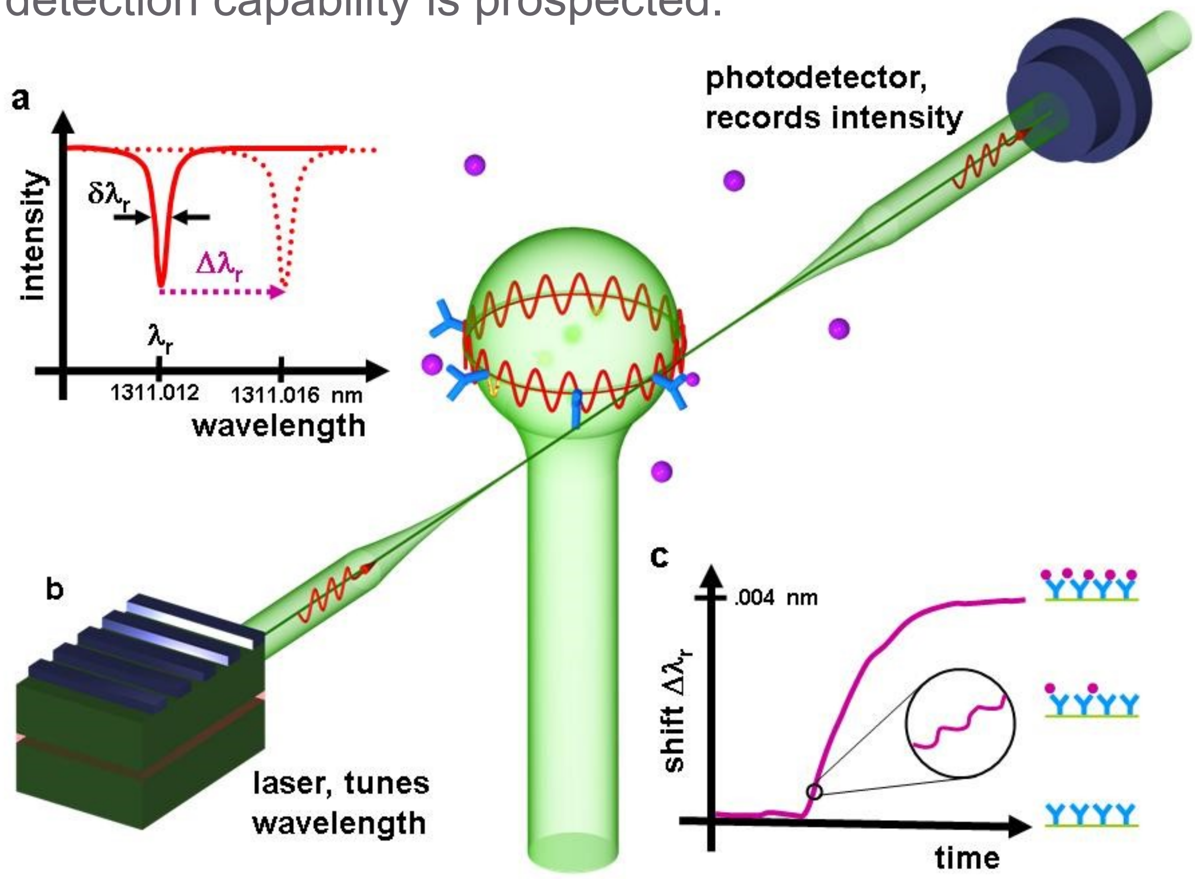

Vollmer group: http://mpl.mpg.de/mpf/php/bfp/research/wgm_biosensing.php

EUROPEAN UNION
European Structural and Investment Funds
Operational Programme Research, Development and Education

MINISTRY OF EDUCATION, YOUTH AND SPORTS

FZU Institute of Physics of the Czech Academy of Sciences

AIT AUSTRIAN INSTITUTE OF TECHNOLOGY

Q-factor and Figure of Merit - FOM

- **Q-factor**: the ratio of the initial energy stored in the resonator to the energy lost in one cycle of oscillation. Can reach 10^6.

$$Q = f/\Delta f = \lambda_{res}/\Delta\lambda$$

- **Figure of merit**: the ratio refractive index sensitvity and resonance width. Can reach $1\text{-}10^3$.

$$FOM = S_b / \Delta\lambda = \left(d\lambda_{res} / d\lambda\right) / \Delta\lambda$$

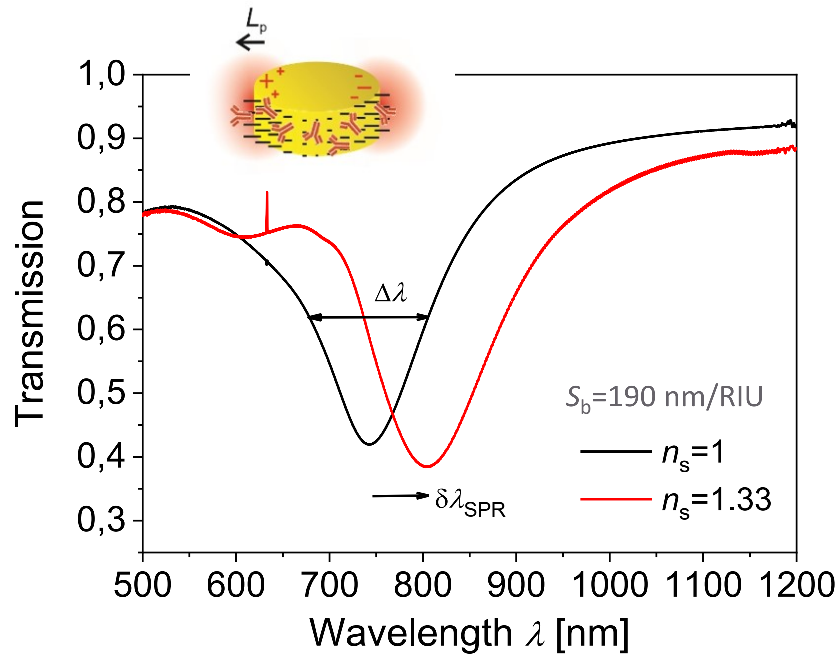

A. Bozdogan, S. Hageneder, J. Dostalek, Plasmonic biosensors relying on biomolecular conformational changes: Case of odorant binding proteins, Methods in Enzymology, Elsevier (2020), ISSN 0076-6879.

Reflectometric Interference Spectroscopy - RIFS

EUROPEAN UNION
European Structural and Investment Funds
Operational Programme Research, Development and Education

MINISTRY OF EDUCATION, YOUTH AND SPORTS

FZU Institute of Physics of the Czech Academy of Sciences

AIT AUSTRIAN INSTITUTE OF TECHNOLOGY

Reflectometric Interference Spectroscpopy (RIfS)

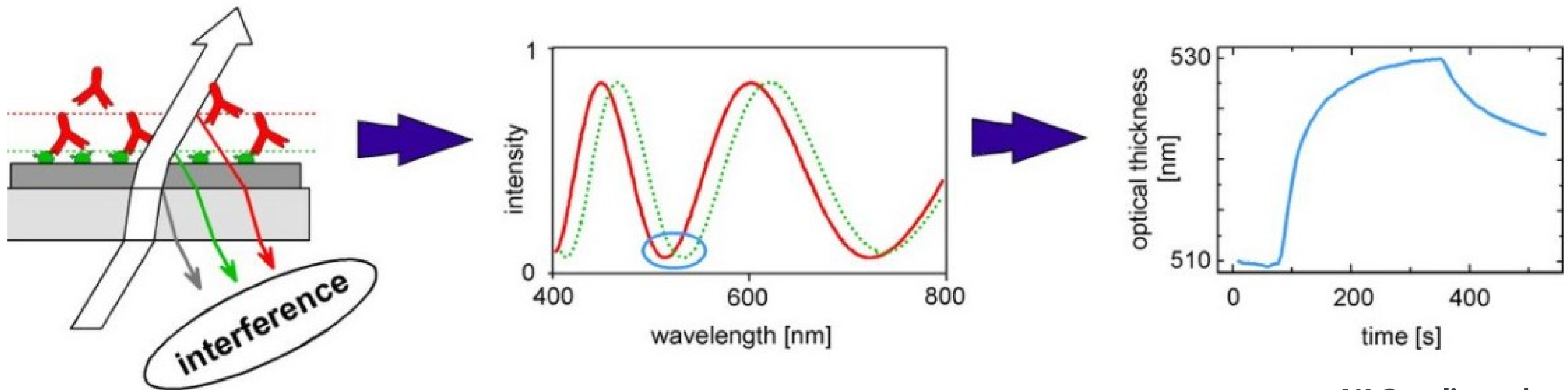

AK Gauglitz webpage

- Fabry-Perot interference on thin dielectric film.
- Very simple chips that do not require structuring to couple light to waveguide resonances. Arguably lower accuracy.

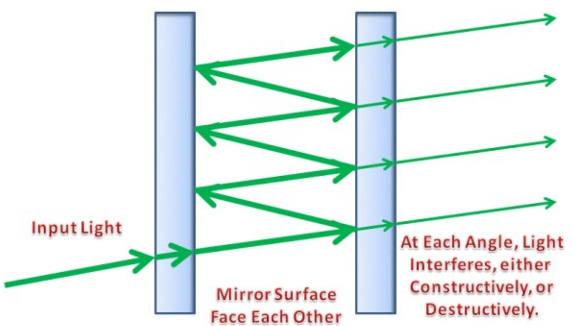

Brecht, A. and Gauglitz, G. (1994) Optimised layer systems for inunumosensors based on the RIfS transducer. *Fresenius J. Anal. Chem.* 349: 360–366., 10.1007/BF00326600

Bio-Layer Interferometry - BLI

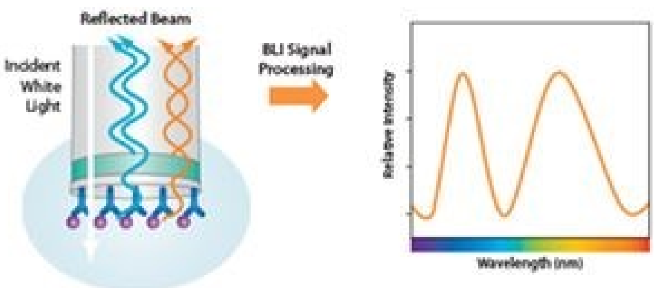

https://www.sartorius.com/en/applications/life-science-research/label-free-detection/bli-technology

- RIfS implemented to fiber optics probes and commercialized by Fortebio, sold as OCTET.
- Used in conjunction with microtiter plates for sequential biomolecular interaction studies.

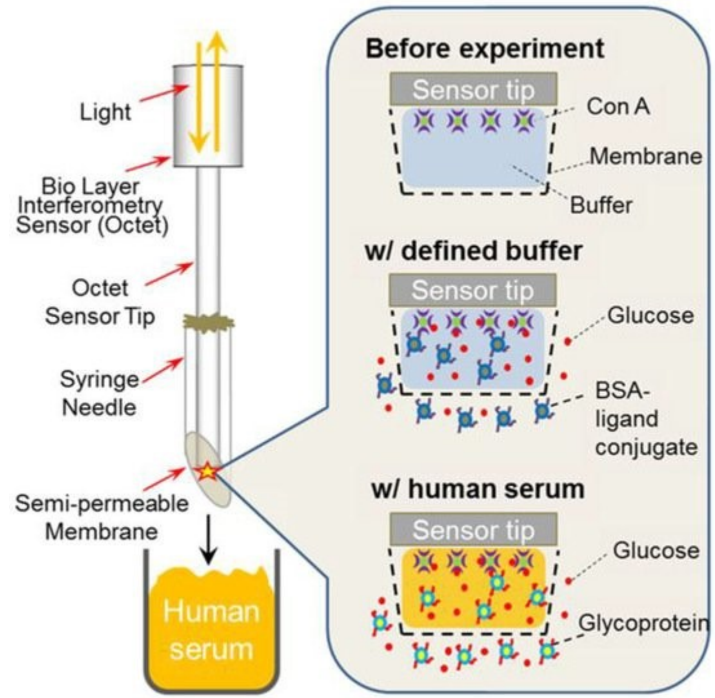

Integration to needles, originally pursued (and dropped) by BIAcore for SPR fiber optic probes.

Seo, D.; Paek, S.-H.; Oh, S.; Seo, S.; Paek, S.-H. A human serum-based enzyme-free continuous glucose monitoring technique using a needle-type bio-layer interference sensor. *Sensors* **2016**, *16*, 1581.

Imaging of Microarrays

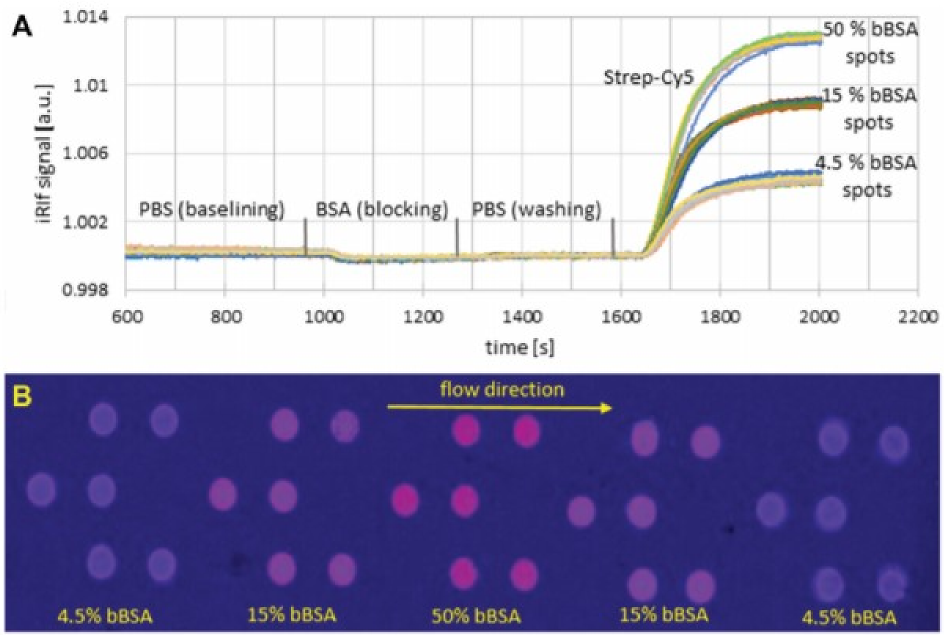

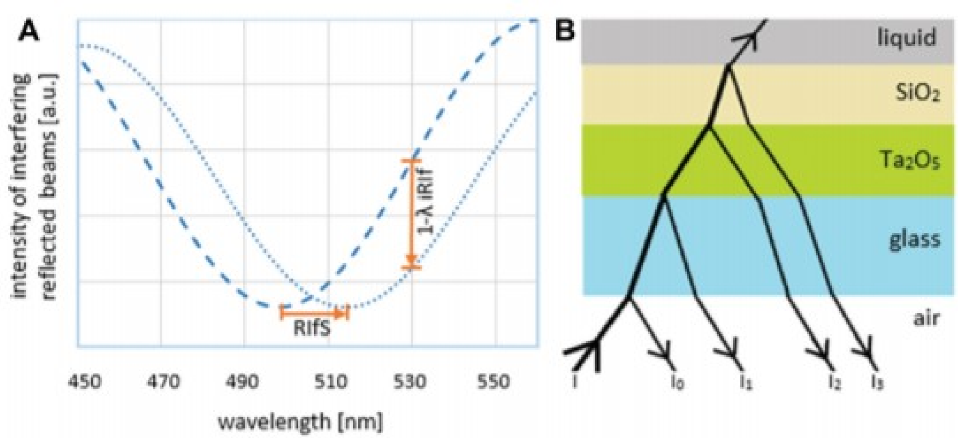

- 1λ–imaging reflectometric interferometry (iRIf) derived from RIfS.
- Argument of advantage with respect to SPR based on the absence of the sensitivity to bulk refractive index and temperature drift.

•10.1177/2211068216657512

Mach Zehnder Interferometry

Rib Waveguide Structure

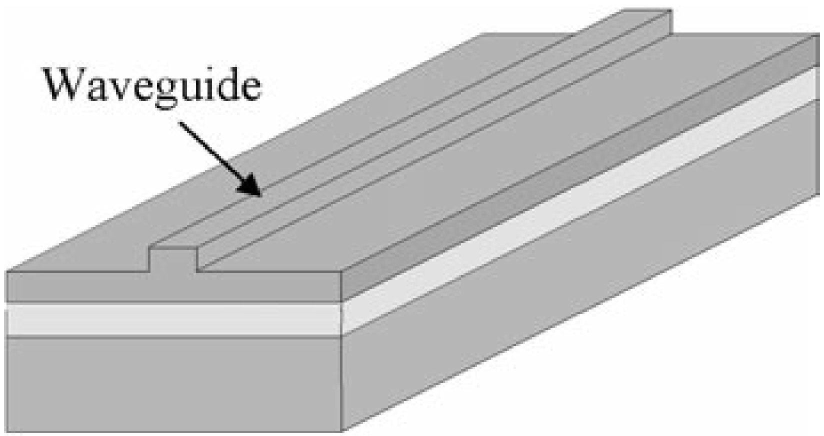

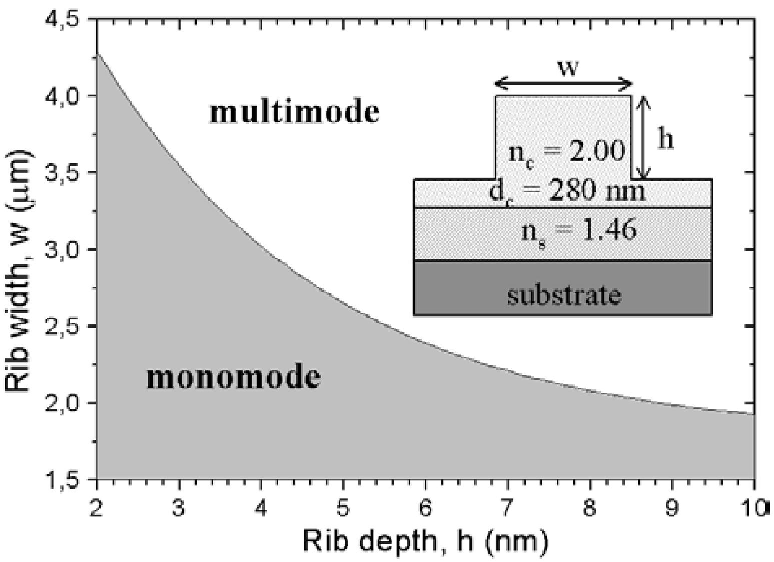

- Rib dielectric structure can be designed to serve as a single mode waveguide, for sufficiently small height

• 10.1177/2211068216657512

Mach Zehnder Interferometer (MZI)

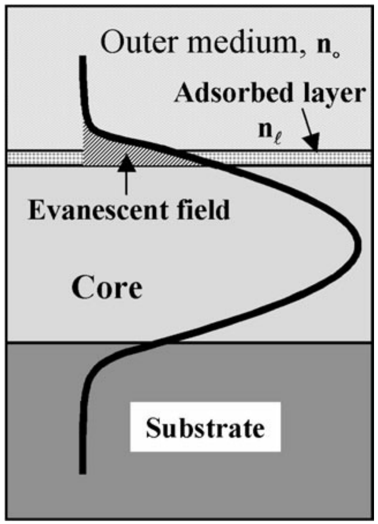

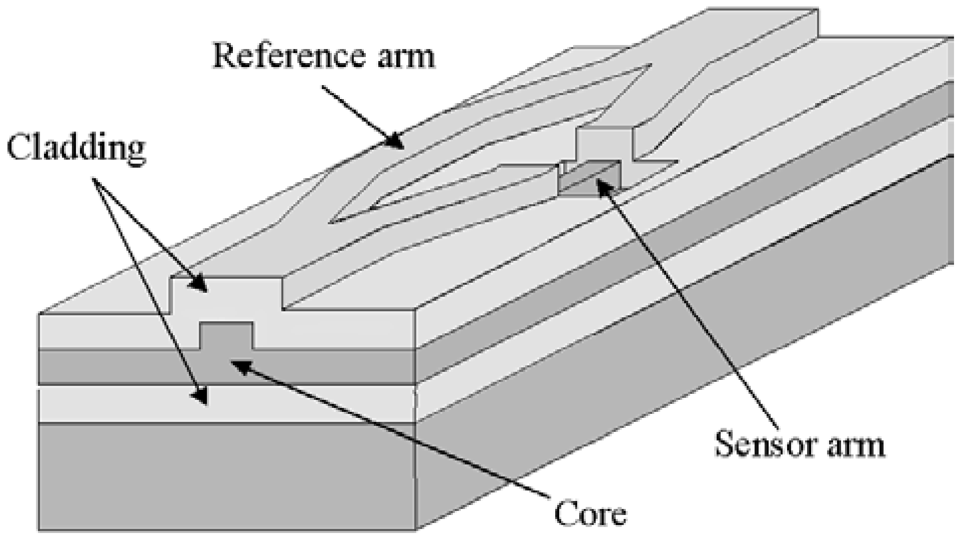

https://doi.org/10.1088/0957-4484/14/8/312

- MZI can be implemented by using integrated optical waveguide structure.
- Phase shift between the reference and measuring (sensor) arm is detected due to the affinity binding events.

EUROPEAN UNION
European Structural and Investment Funds
Operational Programme Research,
Development and Education

MINISTRY OF EDUCATION,
YOUTH AND SPORTS

FZU Institute of Physics of the Czech Academy of Sciences

AIT AUSTRIAN INSTITUTE OF TECHNOLOGY

Interference

Optical phenomenon arising from (coherent) superimposing of amplitudes of two spatially overlapping waves. When changing a phase φ of one of the waves, intensity is varied.

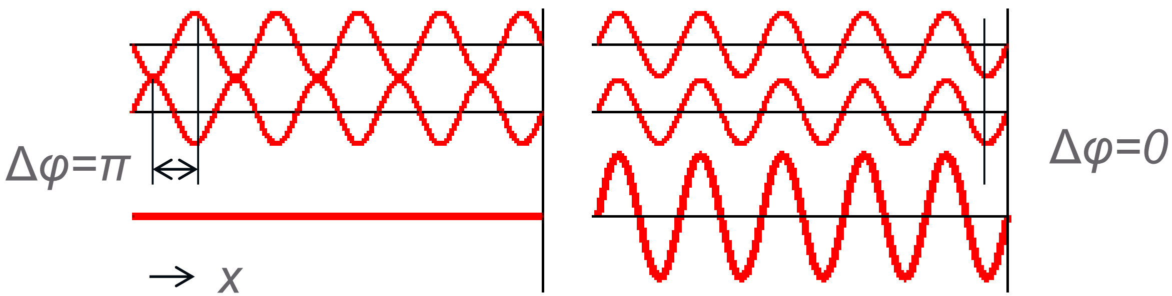

Field amplitudes are subtracted – <u>destructive interference</u>

Field amplitudes are added – <u>constructive interference</u>

$\Delta\varphi=k_0nd$ – a minute changes in refractive index shifts the phase and alters the intensity

$$u(x,t) \propto \sin(k_0nx - \omega t)$$

Exploited in (arguably) most sensitive optical measurements: Frequency stabilized lasers for metrology, microscopy with phase contrast, narrow optical filters,…

EUROPEAN UNION
European Structural and Investment Funds
Operational Programme Research,
Development and Education

Imaging of Microarrays

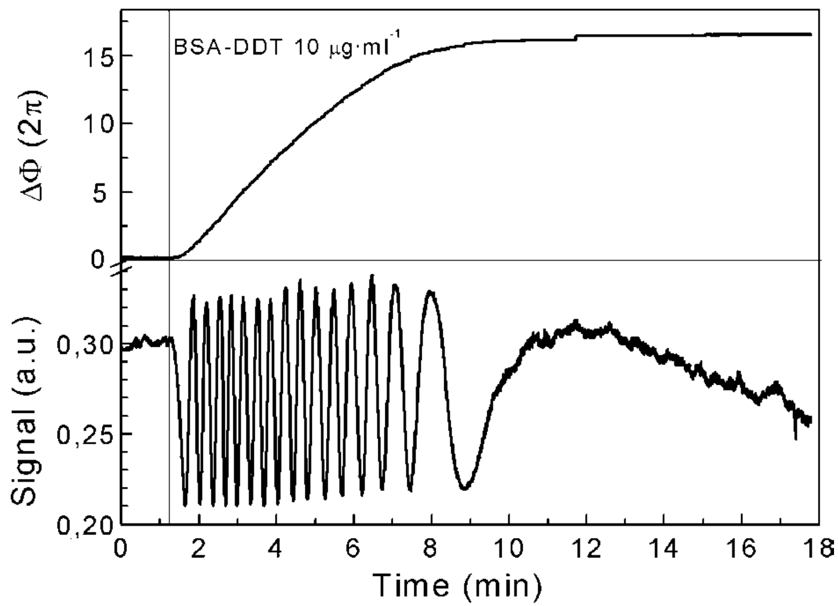

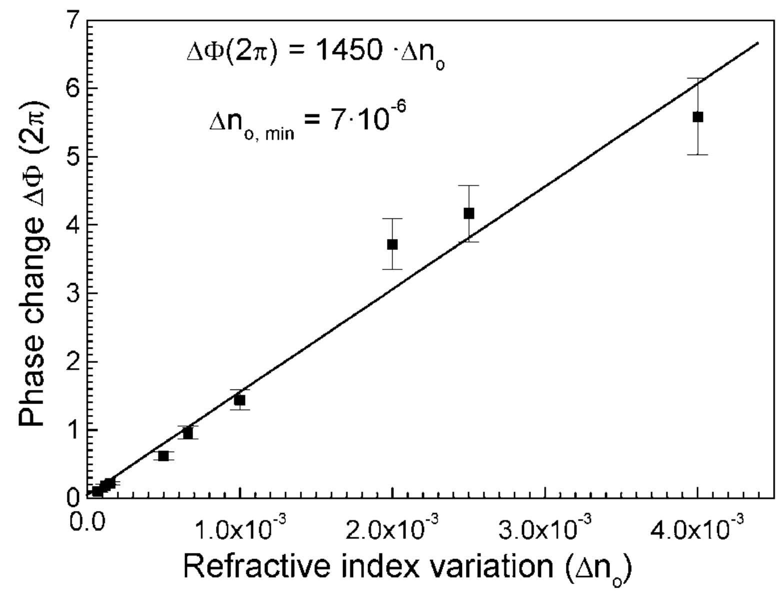

https://doi.org/10.1088/0957-4484/14/8/312

- Example of measured signal and reconstruction of the phase shift due to the protein monolayer growth and bulk refractive index changes.

Multiplexing MZI

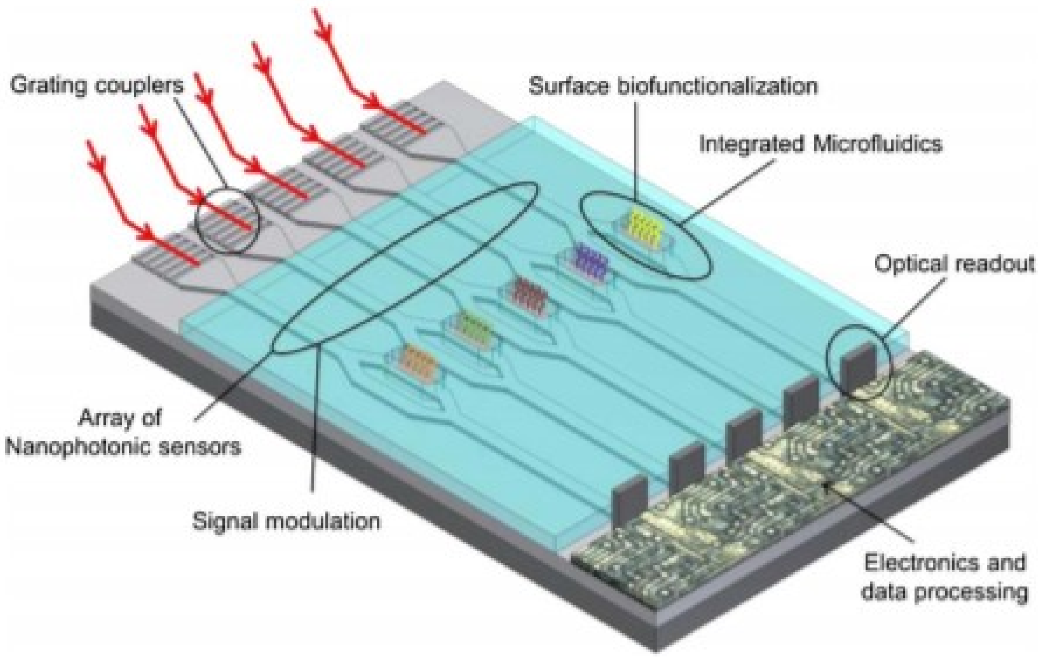

10.1109/JPHOT.2013.2251873

- In general, integrated optics holds potential for highly multiplex measurements through chips with many parallel waveguides.

Increasing Sensitivity

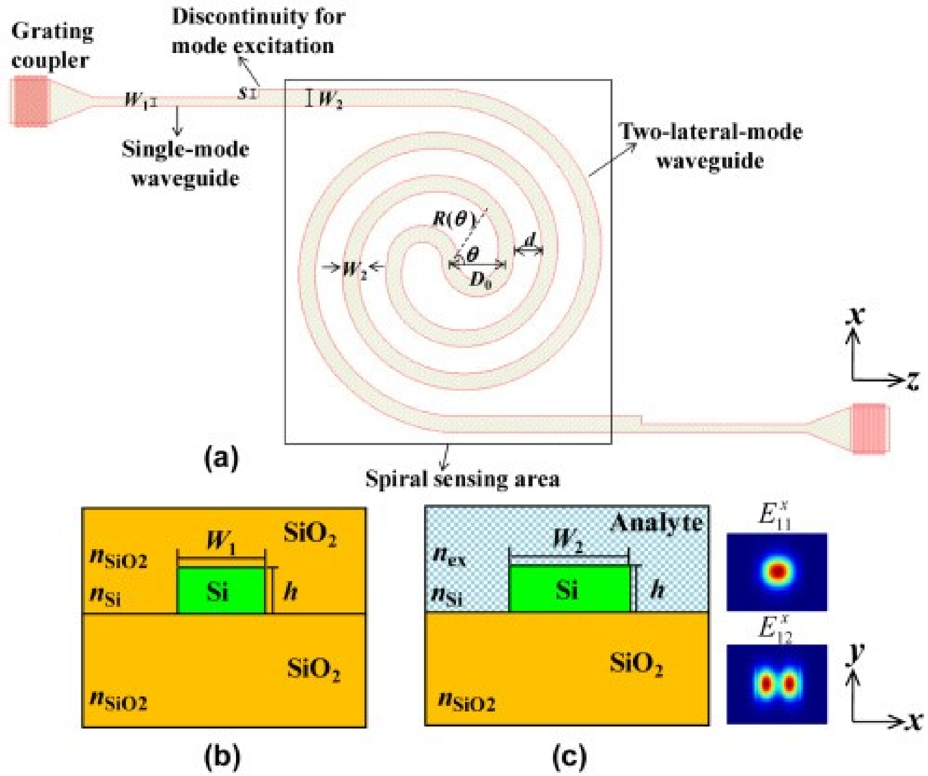

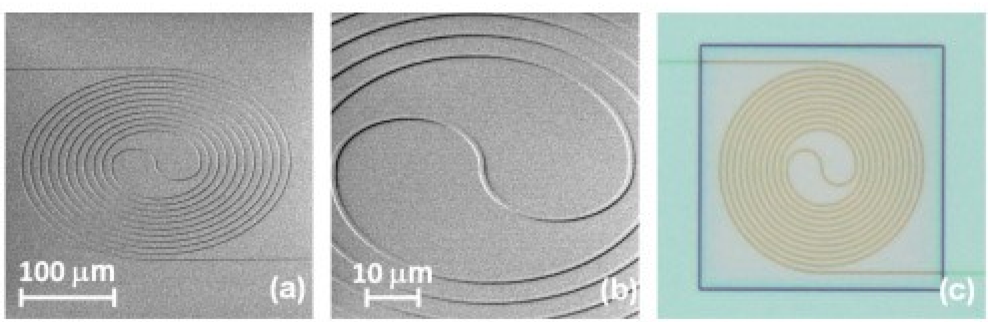

- The phase shift is proportional to the length of the sensor arm section, where the interaction occurs.
- Increasing the length by using of spiral-shaped waveguide structures has been investigated

https://doi.org/10.1364/OE.22.027910

Ring Resonators

Related to MZI, where ring structure enables to cycle light through the sensing arm and accumulate the phase shift.

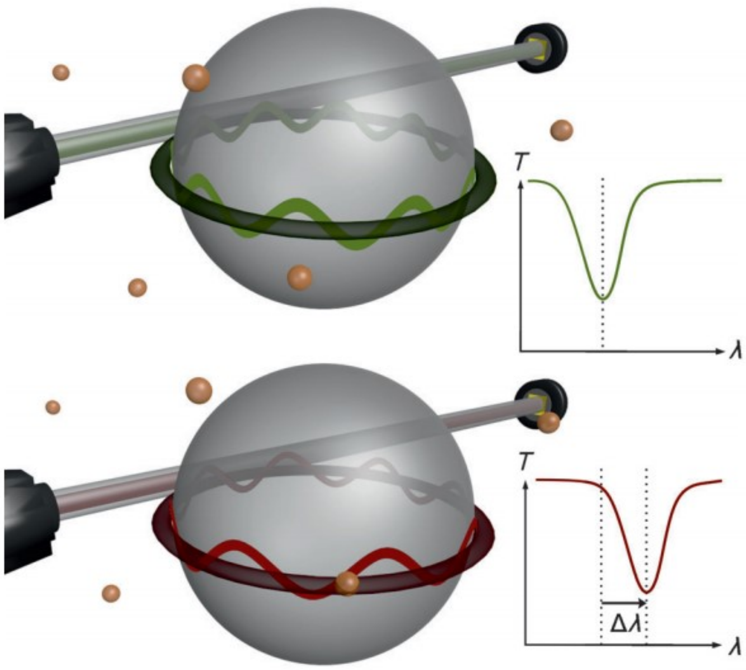

Martin Baaske and Frank Vollmer,
ChemPhysChem 2012, 13, 427 – 436

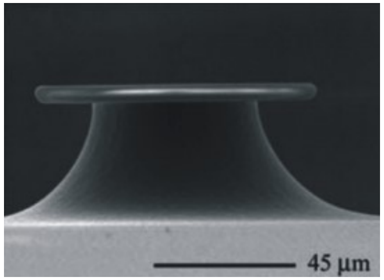

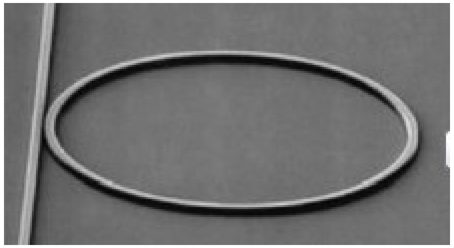

Analytica Chimica Acta
Volume 620, Issues 1–2, 14 July 2008, Pages 8–26

Scattering-Based Detection

Surface Plasmon-Enhanced Scattering

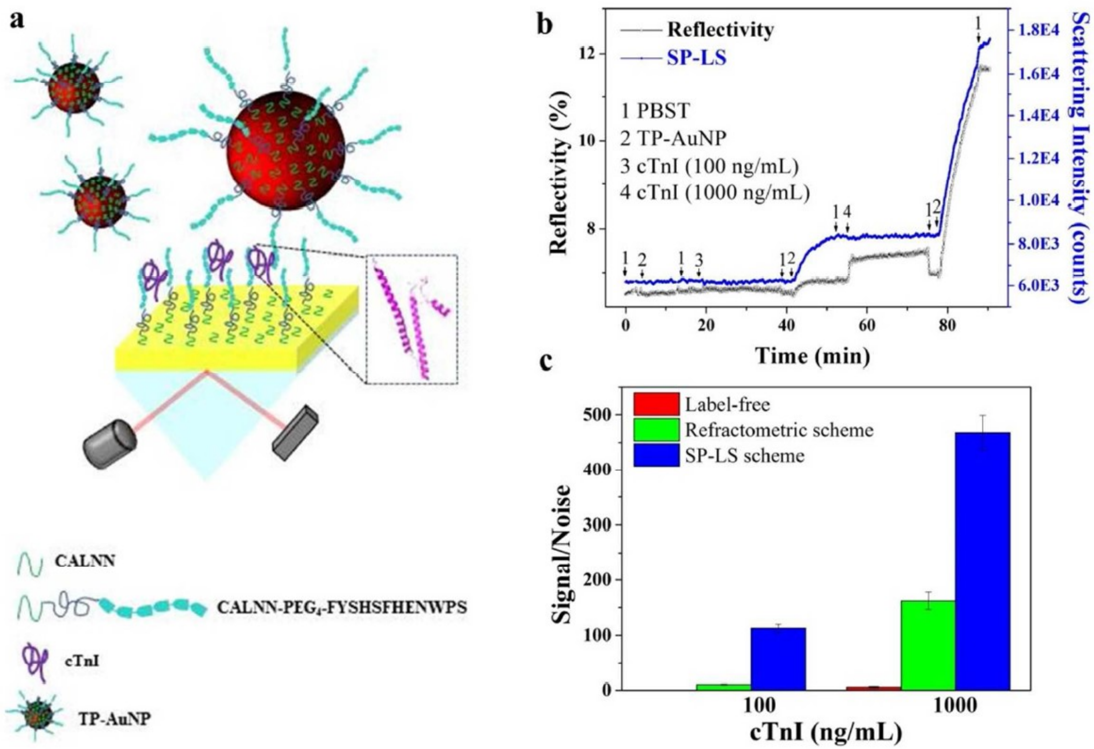

10.1021/acs.analchem.6b03798

- Enhanced intensity of weak scattered signal by probing with intense surface plasmon field

Surface Plasmon-Enhanced Scattering

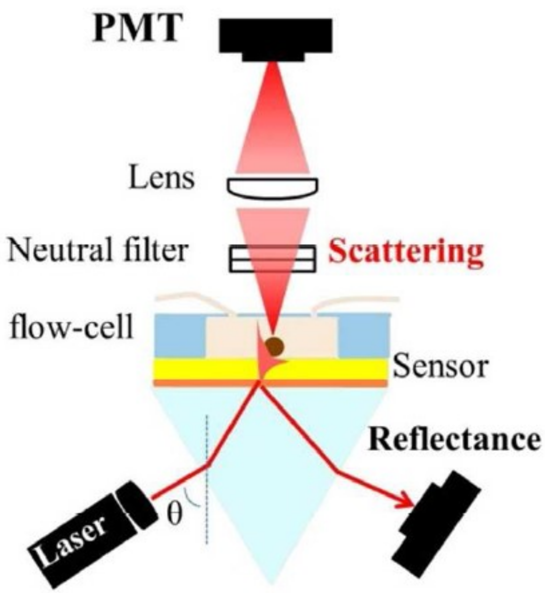

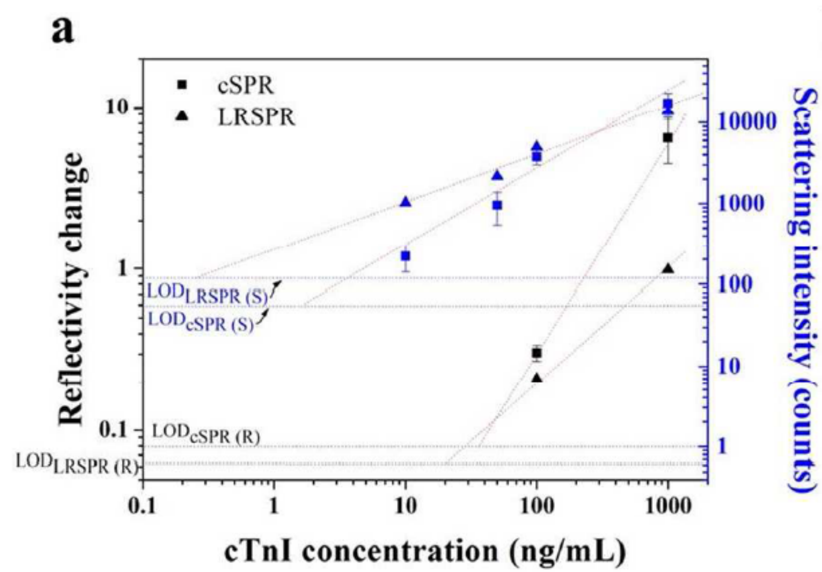

10.1021/acs.analchem.6b03798

- Demonstrated to provide superior limit of detection with respect to classical SPR biosensor approach when used for readout of sandwich troponin assay.

Direct Detection of Scattering

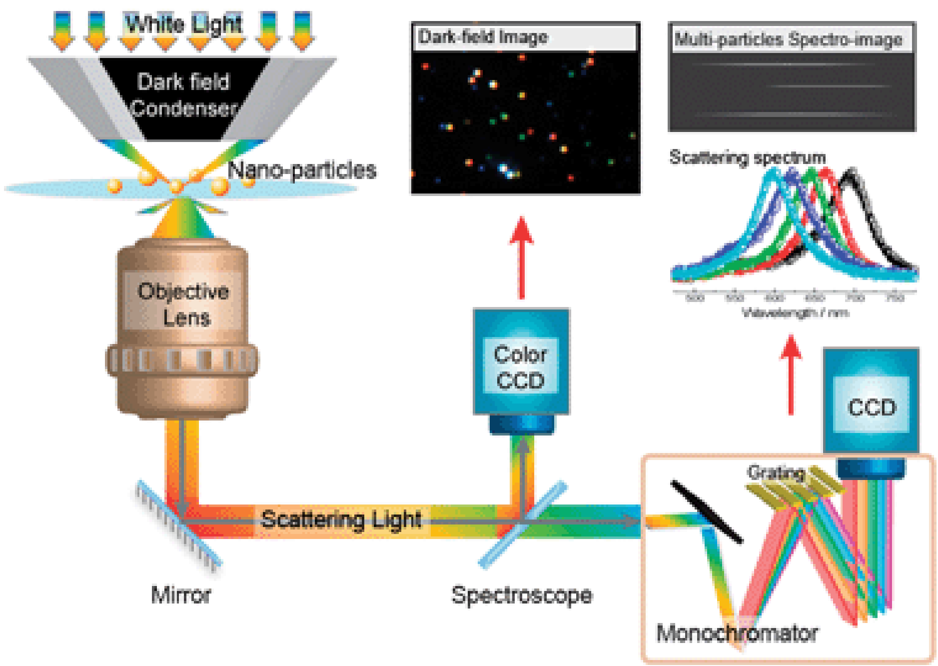

https://doi.org/10.1039/C1CS15143F

- Dark field microscopy enables rather easily observing individual plasmonic nanoparticles.

ISCAT – Interferometric Scattering Microscopy

10.1021/acs.nanolett.9b01822

EUROPEAN UNION
European Structural and Investment Funds
Operational Programme Research,
Development and Education

MINISTRY OF EDUCATION,
YOUTH AND SPORTS

FZU Institute of Physics of the Czech Academy of Sciences

AUSTRIAN INSTITUTE OF TECHNOLOGY

Scattering by Miniature Dielectric Particle

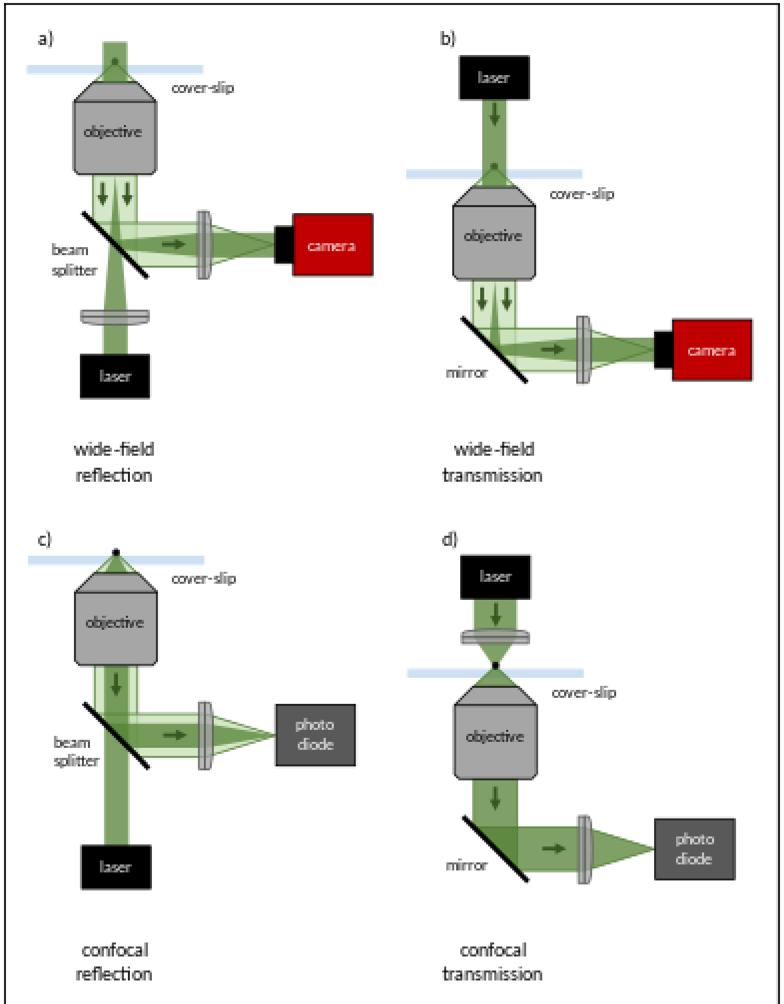

https://en.wikipedia.org/wiki/Interferometric_scattering_microscopy

Rayleigh scattering:

$$\sigma_{\mathrm{sca}} = \frac{8}{3}\pi^2 |\alpha|^2 (\lambda_m)^{-4}$$

Polarizibility of (dielectric) particle

$$\alpha = 3\epsilon_{\mathrm{m}} V \left(\frac{\epsilon_{\mathrm{p}} - \epsilon_{\mathrm{m}}}{\epsilon_{\mathrm{p}} + 2\epsilon_{\mathrm{m}}} \right)$$

ε_p Permittivity of particle

ε_m Permittivity of surrounding medium

Scattering-based Observation of Virus Particles

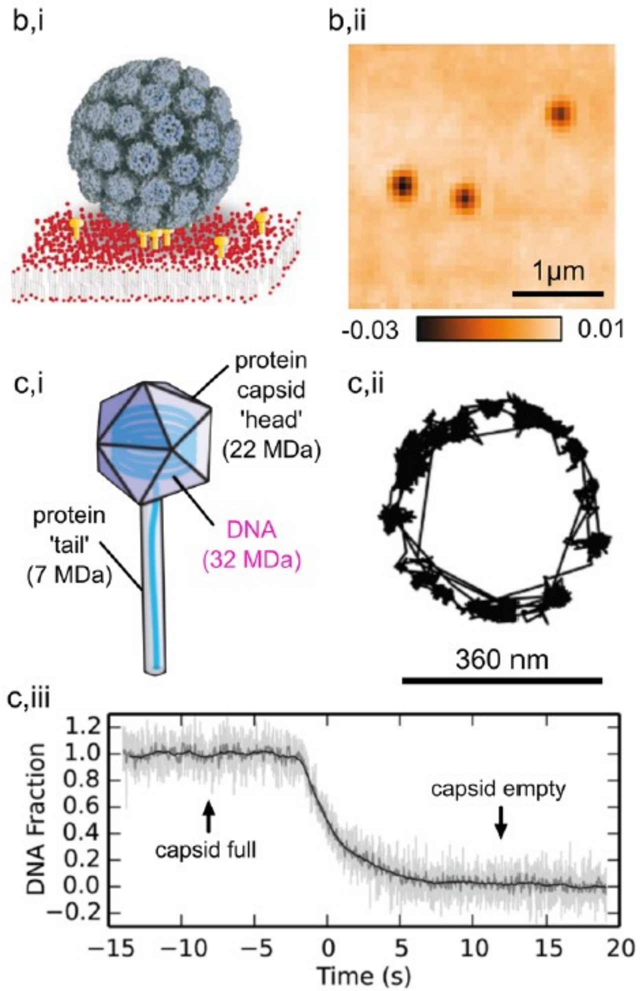

- Direct label-free observation of time dependent rotation of attached virus.
- Release of DNA cargo from the virus.

Figure 2 Illustration of a SV40 virus bound to ganglioside (GM1)-tagged lipids in an artificial lipid bilayer (b,i). An iSCAT image of single SV40 virions attached to a lipid bilayer on a coverslip (b,ii), adapted from ref 22. Illustration of a bacteriophage showing head and tail geometry (c,i). A trajectory from the head of a single bacteriophage whereas its tail is adsorbed to the surface (c,ii). Following stimulation, the DNA content of the capsid head is ejected over time (c,iii), as determined through the diminishing iSCAT contrast. Adapted from ref 44.

Kukura, P.; Ewers, H.; Müller, C.; Renn, A.; Helenius, A.; Sandoghdar, V. Highspeed nanoscopic tracking of the position and orientation of a single virus. Nat. Methods 2009, 6, 923–927.

Scattering by Individual Protein Molecules

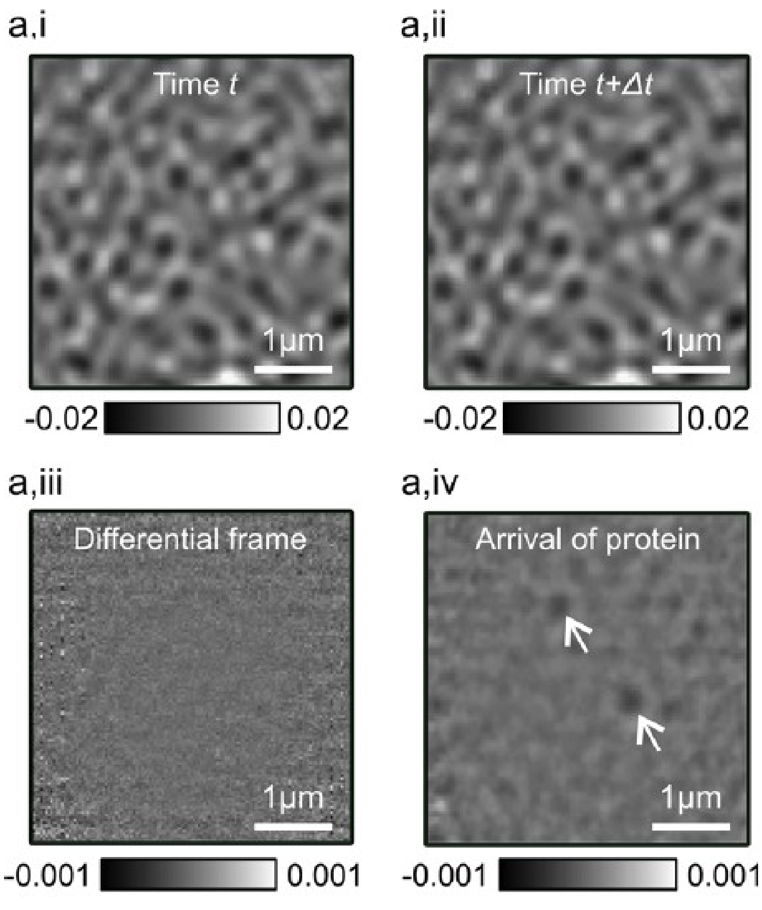

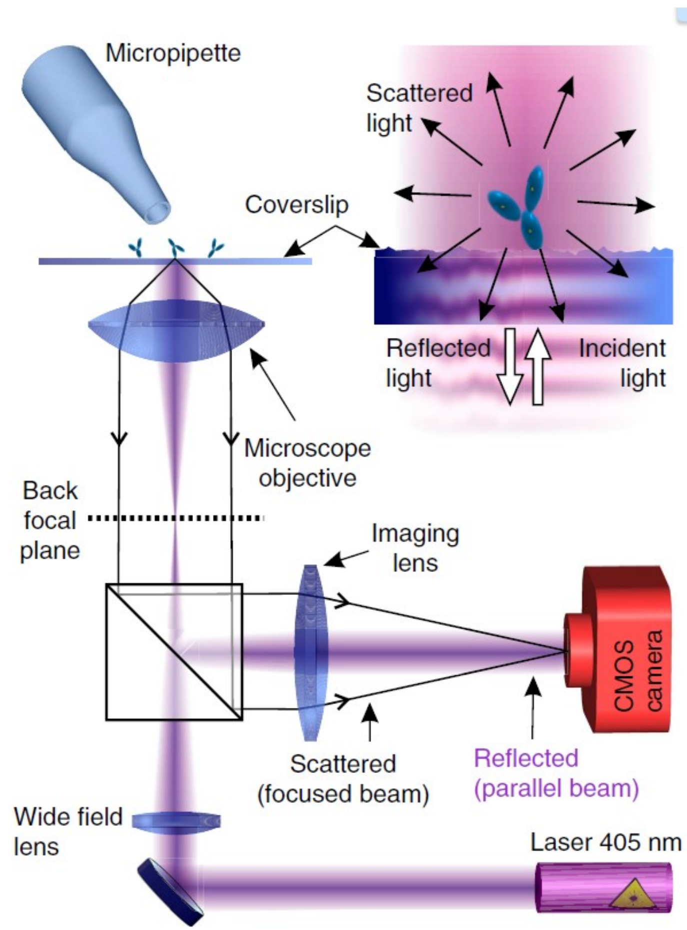

10.1038/ncomms5495